

Pair correlation functions in mixtures of Lennard-Jones particles

Arieh Ben-Naim^{a)} and Raymond Mountain

Physical and Chemical Properties Division, NIST, 100 Bureau Drive Stop 8380, Gaithersburg, Maryland 20899, USA

(Received 1 February 2008; accepted 30 April 2008; published online 3 June 2008)

The pair correlation functions for a mixture of two Lennard-Jones particles were computed by both the Percus-Yevick equations and by molecular dynamics. The changes in the pair correlation function resulting from changes in the composition of the mixtures are quite unexpected. Essentially, identical changes are obtained from the Percus-Yevick equations and from molecular dynamics simulations. The molecular reason for this unexpected behavior is discussed. © 2008 American Institute of Physics. [DOI: 10.1063/1.2931940]

I. INTRODUCTION

More than 30 years ago, one of us (A.B.) examined the form of the pair correlation functions $g_{ij}(R)$ in mixtures of Lennard-Jones (LJ) particles.¹ It was found that when the mole fraction x_A changes from $x_A=0$ to $x_A=1$, the heights and the locations of the first peak of all the pair correlation functions almost do not change. The location of the first peak of $g_{\alpha\beta}(R)$ is roughly at $\sigma_{\alpha\beta}$, where $\sigma_{\alpha\beta}$ is the distance of the closest approach between the particles of species α and β , and is almost independent of the composition. On the other hand, the location of the second peak of $g_{\alpha\beta}(R)$ is determined both by $\sigma_{\alpha\beta}$ as well as by the diameter of the particles that are *most likely* to fill the space between α and β , and depends on the composition. For instance, the first peak of $g_{AA}(R)$ is at σ_{AA} . The location of the second peak depends on the composition of the system. For $x_A \approx 1$, (almost pure A), the second peak occurs at $\sigma_{AA} + \sigma_{AA}$ (see Fig. 1); on the other hand, for $x_A \approx 0$ (A diluted in B), the second peak of $g_{AA}(R)$ occurs at $\sigma_{AA} + \sigma_{BB}$. The height of the second peak was found to change unexpectedly when the composition is changed from $x_A \approx 1$ to $x_A \approx 0$. Instead of shifting gradually from a peak at $2\sigma_{AA}$ to a peak at $\sigma_{AA} + \sigma_{BB}$, it was found that the height of the maximum at $2\sigma_{AA}$ diminishes gradually as x_A decreases, while at the same time a new peak is built up at $\sigma_{AA} + \sigma_{BB}$, reaching a maximal height at $x_A \approx 0$. In the course of writing a new monograph on the “molecular theory of solutions,”² these calculations were repeated and extended for LJ particles of different diameters: $\sigma_{AA}=1$ and $\sigma_{BB}=1.5$, $\sigma_{AA}=1$ and $\sigma_{BB}=2$, and $\sigma_{AA}=1$ and $\sigma_{BB}=3$. In all of these cases, the same kind of changes in the pair correlation functions at the second peak was observed. In this article, we report on a similar study where the pair correlation functions were calculated by both the Percus-Yevick (PY) equations and by molecular dynamics (MD) simulations. The results obtained are not only interesting in themselves, but they also provide further demonstration of the capability of the PY equations to accurately reproduce finer details of the behav-

ior of the pair correlation functions in mixtures.

In Secs. II and III, we describe the model used and the method of calculations of $g_{\alpha\beta}$ based on the PY equations and by MD. In Sec. IV, we compare the results obtained from the two methods. The interpretation of the results is discussed in Sec. V.

II. THE MODEL AND THE METHOD OF CALCULATIONS BY PERCUS-YEVICK EQUATIONS

The calculations for this article were done for LJ particles. Let A and B be two simple spherical molecules interacting through pair potentials which we denote by $U_{AA}(R)$, $U_{AB}(R)$, and $U_{BB}(R)$, of the form

$$U_{\alpha\beta}(R) = 4\epsilon_{\alpha\beta} \left[\left(\frac{\sigma_{\alpha\beta}}{R} \right)^{12} - \left(\frac{\sigma_{\alpha\beta}}{R} \right)^6 \right]. \quad (2.1)$$

We also assume the combination rules

$$\sigma_{AB} = \sigma_{BA} = (\sigma_{AA} + \sigma_{BB})/2, \quad (2.2)$$

$$\epsilon_{AB} = \epsilon_{BA} = (\epsilon_{AA}\epsilon_{BB})^{1/2}. \quad (2.3)$$

The PY equation for pure spherical molecules has the form³

$$y(\bar{R}_1, \bar{R}_2) = 1 + \rho \int_V y(\bar{R}_1, \bar{R}_2) f(\bar{R}_1, \bar{R}_3) \times [y(\bar{R}_2, \bar{R}_3) f(\bar{R}_2, \bar{R}_3) + y(\bar{R}_2, \bar{R}_3) - 1] dR_3, \quad (2.4)$$

where f is the Mayer function defined as

$$f(R) = \exp[-\beta U(R)] - 1 \quad (2.5)$$

and $y(R)$ is defined as

$$y(R) = g(R) \exp[\beta U(R)]. \quad (2.6)$$

Another simpler and useful form of this equation is obtained by transforming to bipolar coordinates

$$u = |\bar{R}_1 - \bar{R}_3|, \quad v = |\bar{R}_2 - \bar{R}_3|, \quad R = |\bar{R}_1 - \bar{R}_2|. \quad (2.7)$$

The element of volume is expressed as

^{a)}Present address: Department of Physical Chemistry, The Hebrew University of Jerusalem, Givat Ram, Jerusalem, Israel. Electronic mail: arieh@fh.huji.ac.il.

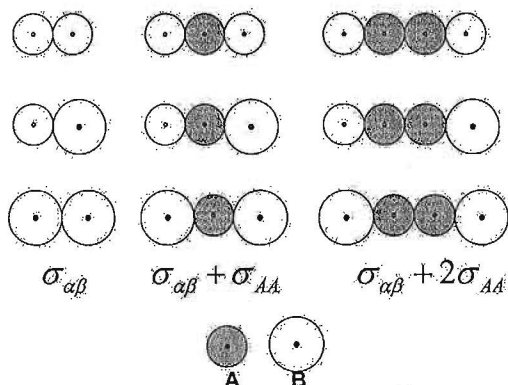


FIG. 1. Configurations corresponding to the first three peaks of $g_{\alpha\beta}(R)$ for a system dominated by A particles. The diameters of the A and the B particles are $\sigma_A=1$ and $\sigma_B=1.5$, respectively. The shaded circles are the particles that are most likely to fill the space between α and β , at this composition ($x_A \approx 1.0$).

$$dR_3 = 2\pi u v d u d v / R \quad (2.8)$$

and Eq. (2.4) is transformed into

$$y(R) = 1 + 2\pi\rho R^{-1} \int_0^\infty y(u)f(u)u du \times \int_{|R-u|}^{R+u} [y(v)f(v) + y(v) - 1]v dv. \quad (2.9)$$

For the numerical solution, it is convenient to transform the PY equation by defining the function²⁻⁶

$$z(R) = y(R)R. \quad (2.10)$$

Hence, we get an integral equation for $z(R)$, which reads

$$z(R) = R + 2\pi\rho \int_0^\infty z(u)f(u)du \times \int_{|R-u|}^{R+u} [z(v)f(v) + z(v) - v]dv. \quad (2.11)$$

For mixtures, of say, two components, Eq. (2.11) is generalized to

$$z_{\alpha\beta}(R) = R + \sum_{\gamma=A,B} 2\pi\rho_\gamma \int_0^\infty z_{\alpha\gamma}(u)f_{\alpha\gamma}(u)du \times \int_{|R-u|}^{R+u} [z_{\gamma\beta}(v)f_{\gamma\beta}(v) + z_{\gamma\beta}(v) - v]dv, \quad (2.12)$$

where the sum includes two terms $\gamma=A,B$. The numerical procedure is similar to the case for one component. One starts with

$$z_{\alpha\beta}(R) = R \quad (2.13)$$

for all the four functions $z_{\alpha\beta}(R)$ and proceeds to solve the four integral equations [Eq. (2.12)] by iteration. (For more details, see Refs. 1 and 2).

III. NPT MOLECULAR DYNAMICS SIMULATIONS

A FORTRAN code that implements the NPT ensemble⁷ was written and tested for a one component LJ fluid. The equation of state generated with this code is in close agreement with the extensive body of simulation results for that system.⁸ The code was then extended to simulate mixtures of LJ particles.

The mixture studies are for 500 particles of two sizes. The smaller type A particle has LJ parameters $\epsilon_{AA}/kT=0.5$ and $\sigma_{AA}=1$ and the larger type B particle has LJ parameters $\epsilon_{BB}/kT=0.5$ and $\sigma_{BB}=1.5$. The mass of the type A particle is set to 1 and that of the type B particle is arbitrarily set to 1.3. The time unit τ is

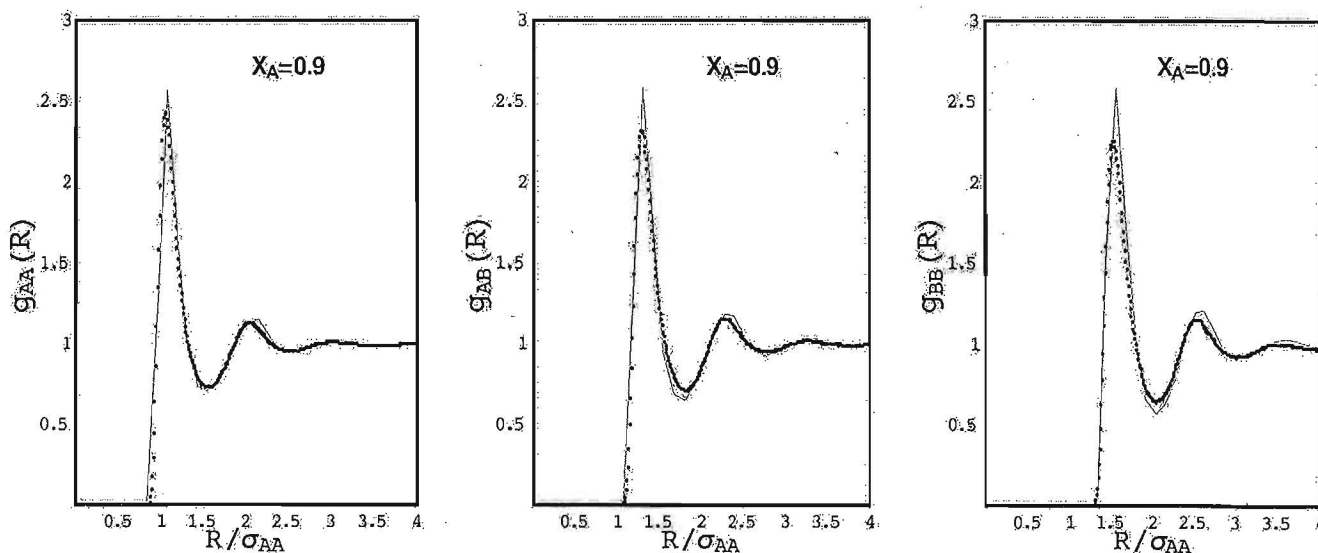


FIG. 2. The pair correlation functions $g_{AA}(R)$, $g_{AB}(R)$, and $g_{BB}(R)$ for $x_A=0.9$. Solid lines from PY equations; Dotted curves from simulations.

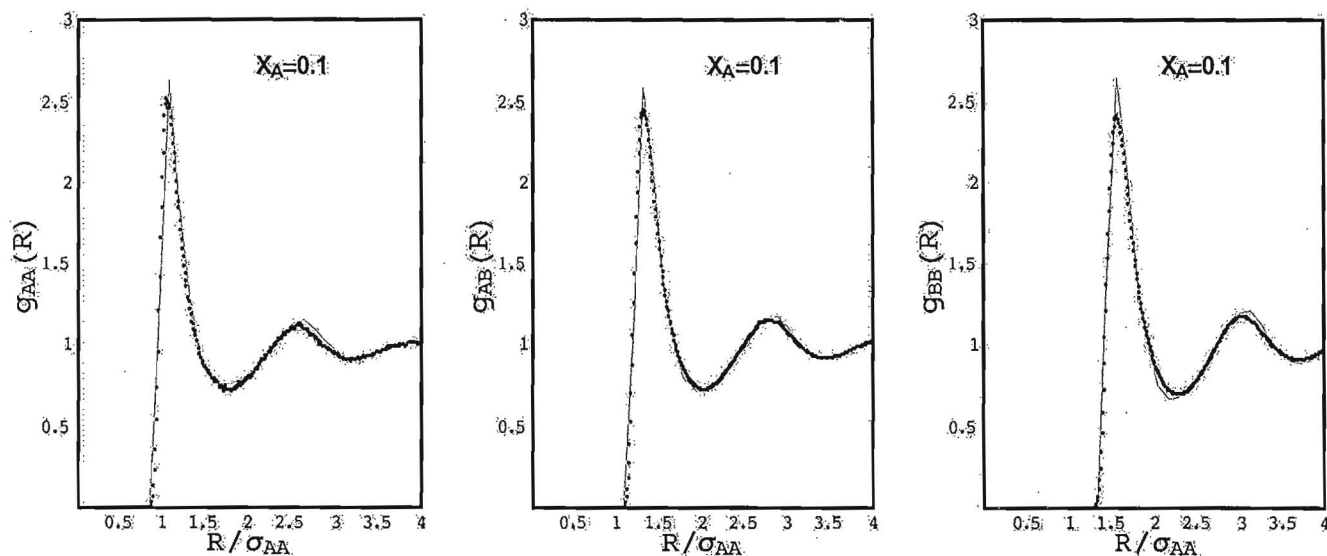


FIG. 3. The pair correlation functions $g_{AA}(R)$, $g_{AB}(R)$, and $g_{BB}(R)$ for $x_A=0.1$. Solid lines from PY equations; same from simulations.

$$\tau = \sqrt{m_{AA}\sigma_{AA}^2/\epsilon_{AA}} = 1. \quad (3.1)$$

The particular set of simulations of interest has a packing fraction

$$\eta = \frac{\pi\rho}{6}(x_{AA}\sigma_{AA}^3 + x_{BB}\sigma_{BB}^3) = 0.45, \quad (3.2)$$

where x_A and x_B are the mole fractions of type A and type B particles, respectively, and $\rho = \rho_A + \rho_B$. A series of states with x_A between 0.1 and 0.9 were generated by adjusting the specified pressure until the volume fraction of $\eta=0.45$ was realized. This typically took three iterations of the system. When the desired volume was obtained, a production run of 1000τ was made with a time step of 0.01τ . The pair correlation functions for the fluid were generated and normalized to unity at large separations.

IV. RESULTS FROM THE PERCUS-YEVICK EQUATIONS AND THE MOLECULAR DYNAMICS SIMULATIONS

In this section, we describe the results obtained by solving the PY equations for LJ particles and by simulation. We shall focus specifically on the variation of $g_{\alpha\beta}(R)$ at the location of the second peak.

The parameters used for these calculations are

$$\sigma_{AA} = 1.0, \quad \sigma_{BB} = 1.5, \quad (4.1)$$

$$\frac{\epsilon_{AA}}{kT} = \frac{\epsilon_{BB}}{kT} = 0.5, \quad \eta = 0.45.$$

We have done the calculation on the following compositions: $x_A=0.1$, $x_A=0.9$, and around $x_A=0.65$. The results are discussed separately for the three regions.

- (1) Systems that are dominated by the presence of A's, between any pair of particles, i.e., $x_A \approx 1$.

Figure 2 shows the three pair correlation functions for a system with composition $x_A=0.9$, obtained by both the PY and the MD methods. At this composition, $g_{AA}(R)$ is

almost identical with the pair correlation function for pure A. The peaks occur at about σ_{AA} , $2\sigma_{AA}$, and $3\sigma_{AA}$. Since $\eta=0.45$ in Eq. (3.2) corresponds to quite a high density, we have three peaks; two pronounced and one weaker peak. The function $g_{AB}(R)$ has the first peak at about σ_{AB} . [The value of σ_{AB} is $(\sigma_{AA} + \sigma_{BB})/2 = 1.25$. However, due to errors in the numerical computation and the fact that the minimum of U_{AB} is at $2^{1/6}\sigma_{AB}$, we actually obtain the first maximum at about $R=1.3$]. The second and the third peaks of $g_{AB}(R)$ are determined not by multiples of σ_{AB} , but by the addition of σ_{AA} . That is, the maxima are at $R \approx \sigma_{AB}$, $\sigma_{AB} + \sigma_{AA}$, $\sigma_{AB} + 2\sigma_{AA}$, etc. This is a characteristic feature of a dilute solution of B in A, where the spacing between the maxima is determined by σ_{AA} , i.e., the diameter of the denominating species. Similarly, the first peak of $g_{BB}(R)$ is at about $\sigma_{BB}=1.5$ and the second and third peaks occur at $\sigma_{BB} + \sigma_{AA}$ and $\sigma_{BB} + 2\sigma_{AA}$, respectively. The molecular reason for this is very simple. The spacing between, say the first and second peaks, is determined by the size of the molecule that will most probably fill the space between the two molecules under the observation. Because of the prevalence of A molecules

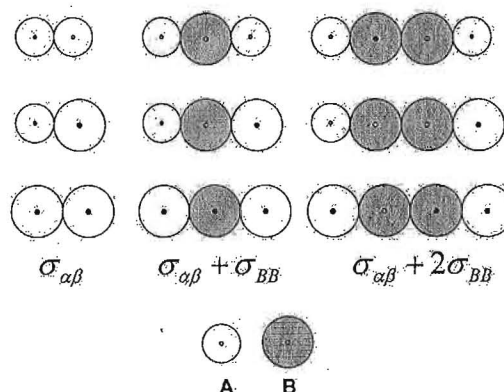


FIG. 4. As in Fig. 1, but for $x_A \approx 0$, i.e., a system dominated by B particles (the shaded circles are the particles filling the space between α and β).

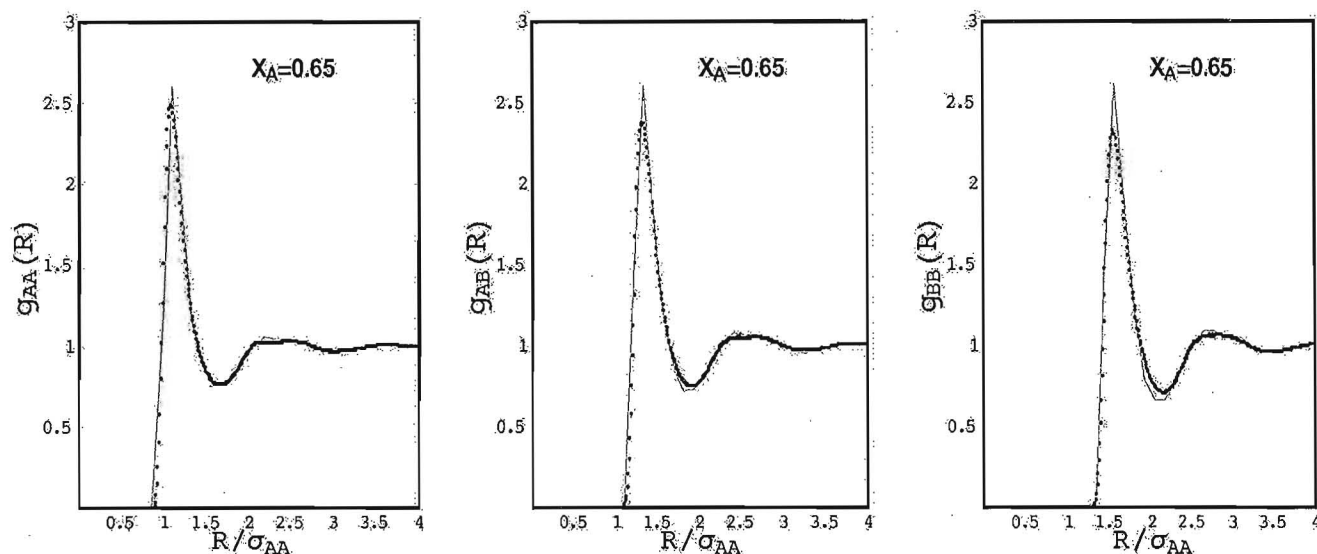


FIG. 5. The pair correlation functions $g_{AA}(R)$, $g_{AB}(R)$, and $g_{BB}(R)$ for $x_A=0.65$. Solid lines from PY equations; dotted curves from simulations.

in this case, they are the most likely to fill the space between A and B. The situation is depicted schematically in Fig. 1 where we show the most likely filling of space between a pair of molecules for the case $x_A \approx 1$, i.e., for a very dilute solution of B in A. The first row shows the approximate locations of the first three peaks of $g_{AA}(R)$; other rows correspond successively to $g_{AB}(R)=g_{BA}(R)$ and $g_{BB}(R)$.

For $x_A \approx 1$, the component A may be referred to as the *solvent* and B as the *solute*. For any pair of species $\alpha\beta$, we can pick up two specific particles (one of species α and the other of species β) and refer to these particles as a “dimer.” From the second row of Fig. 1, we see that the most probable configurations of the dimers occur either when the separation is σ_{AB} or when they are

“solvent separated,” i.e., when the distances are $R \approx \sigma_{AB} + n\sigma_{AA}$, where $n=1,2,3$, for the second, third, and fourth peaks. Note that because of the approximate nature of the computations, the curves $g_{AB}(R)$ and $g_{BA}(R)$ may come out a little different; however, theoretically, they should be identical and in our computation, they are nearly identical and may not be distinguished on the scale of Fig. 2. Note that the results obtained by the PY and the MD are nearly the same as shown in Fig. 2.

- (2) System dominated by the presence of B's, between any pair of particles, i.e., $x_A \approx 0$ or $x_B \approx 1$.

This is the other extreme case where $x_A \approx 0$ or $x_B \approx 1$. Figure 3 shows the pair correlation functions for this case obtained by the two methods. Here A is diluted in B and the separation between the peaks is determined by σ_{BB} , since now it is B that dominates the space between any pair of particles. Thus, the first peak of $g_{AA}(R)$ appears at σ_{AA} as expected. However, the second and third peaks are roughly at $\sigma_{AA} + \sigma_{BB}$ and $\sigma_{AA} + 2\sigma_{BB}$, respectively.

Figure 4 shows the configurations corresponding to first three peaks of $g_{\alpha\beta}(R)$ for the system of A diluted in B. Note that in this case, it is in the B particles that are most likely to fill the space between the pair of particles for which $g_{\alpha\beta}(R)$ is under consideration.

- (3) Systems of intermediate composition: $x_A \approx 0.65$.

Figure 5 shows the pair correlation functions $g_{\alpha\beta}(R)$ for the composition $x_A=0.65$. A remarkable feature of these curves is the almost complete disappearance of the third and fourth peaks. The second peak has developed a broad, nearly flat region unlike the case of either $x_A=0.9$ or $x_A=0.1$. Since no component is dominant in this case, we cannot describe the most likely configuration as we did in Figs. 1 and 4. A magnified view of the second peak for region $g_{AA}(R)$ is provided in Fig. 6 where the MD results are shown for $x_A=0.7$ (dash-dot line), $x_A=0.65$ (dashed line), and $x_A=0.6$ (solid line). In this composition interval the position of the second

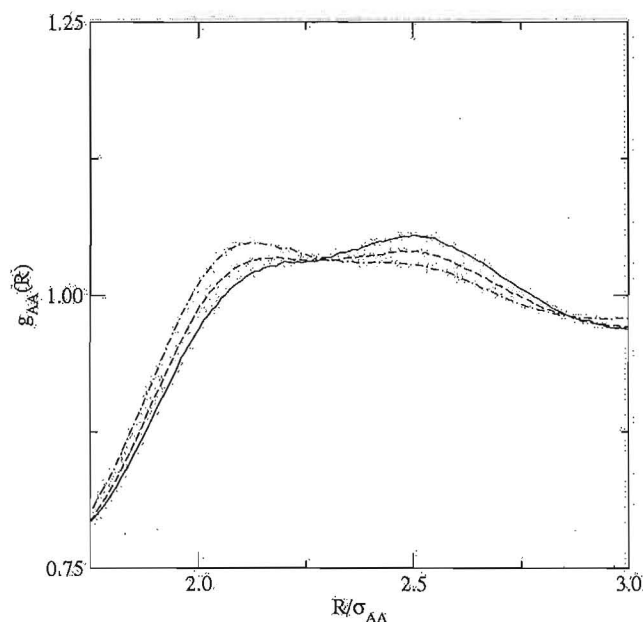


FIG. 6. The pair correlation function $g_{AA}(R)$ for $x_A=0.7$ (dashed dot line), 0.65 (dashed line), and 0.6 (solid line). Only the region between $1.75 \leq R \leq 3$ is shown.

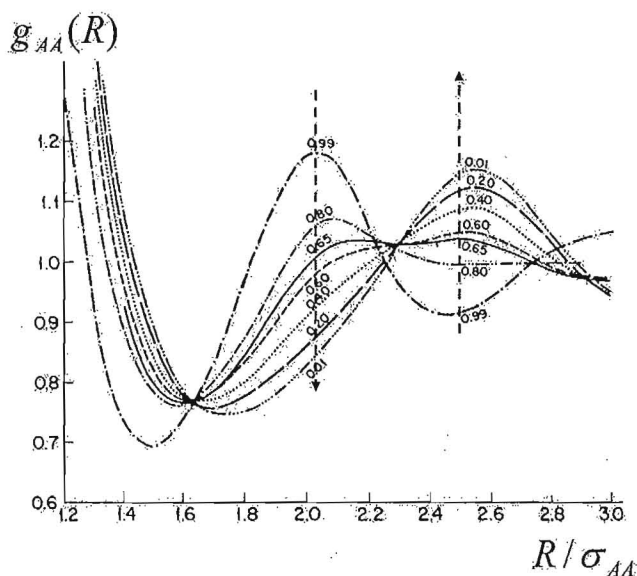


FIG. 7. A magnified view of the second peak of $g_{AA}(R)$ is shown as a function of the mole fraction of component A (indicated by the numbers on the curves). The arrows indicate how the amplitudes at 2.0 and 2.5 changes as the mole fraction of A changes from 0.99 to 0.01 (taken from Ref. 1).

maximum in $g_{AA}(R)$ shifts from about $\sigma_{AA} + \sigma_{BB}$ at $x_A = 0.6$ to about $\sigma_{AA} + \sigma_{AA}$ at $x_A = 0.7$. There are corresponding changes in the position of the second peak in $g_{AB}(R)$ and $g_{BB}(R)$. The PY results show the same behavior as the MD results. A more detailed behavior of the pair correlation function near the second peak is shown in Fig. 7.

V. DISCUSSION

As it is well known,^{1,2} the second and the third peaks of the pair correlation function disappear when the volume density is low. This is true for all compositions. The phenomena we have observed in the mixture at a relatively high volume density ($\eta = 0.45$) is not a result of the scarcity of particles in the system but a result of the competition between the species A and B to occupy the space between the two selected particles.

We recall that the location of the second peak is determined principally by the size of the particles that fill the space between the two selected particles. For $x_A = 0.9$, it is most likely that the space will be filled by A molecules (Fig. 1). Similarly, for $x_A = 0.1$, it is most probable that the B molecules will be filling the space (Fig. 4). The strong second peak of $g_{AA}(R)$ at $2\sigma_{AA}$ in the first case and at $\sigma_{AA} + \sigma_{BB}$ in the second case reflects the high degree of certainty with which the system chooses the species for filling the space between any pair of selected particles. As the mole fraction of A decreases, the B molecules become competitive with A for the “privilege” of filling the space. At about $x_A \approx 0.65$, B is in a state of emulating A (in the sense of filling the space). The fact that this occurs at $x_A \approx 0.65$ and not, say at $x_A \approx 0.5$ is a result of the difference in the diameters of the two components. In our case, the ratio $\sigma_{AA}/\sigma_{BB} = 1/1.5 \approx 0.66$. The flattening of the second peak reflects the inability of the

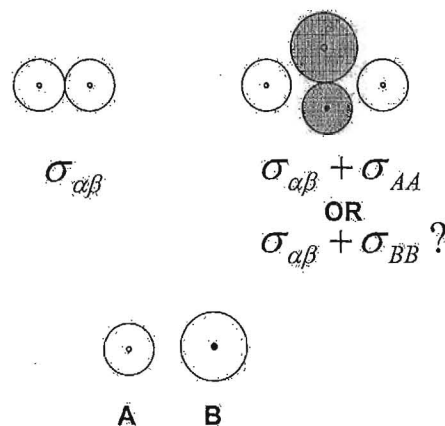


FIG. 8. Schematic description of the locations of the first peak (at contact), and the disappearance of the location of the second peak when there exists no dominating molecules to fill the space between the two particles.

system to “make a decision” as to which kind of particle should be filling the space between the two selected particles. This is shown schematically in Fig. 8.

The flattening of the second peak can be interpreted also in terms of the solvent induced force between the two particles in the mixture. For the LJ particles discussed in this article, the potential of mean force is related to the pair correlation functions by

$$W_{\alpha\beta}(R) = -kT \ln g_{\alpha\beta}(R).$$

At distances of $R \geq 2$, the direct forces are negligible for all compositions. However, for either $x_A \approx 0.1$ or $x_A \approx 0.9$, and for $\eta \approx 0.45$, there exists a significant solvent-induced force between α and β . The flattening of the pair correlation functions at the location of the second peak can be interpreted in terms of almost no solute-induced force between the pair of particles α and β . Note however, that although the pair correlation functions are nearly flat at the region of the second peak, the values of $g_{\alpha\beta}(R)$ in this region is not unity. Thus, the correlation is small but finite, while the solvent induced force is nearly zero in this region.

The fact that the results from the PY and the simulations agree both qualitatively and quantitatively, evidently shows that the PY approximation is valid, and can reproduce these fine details of the behavior of the pair correlation functions in mixtures.

We conclude with two notes regarding the phenomenon reported in this article. First, it was brought to our attention by the referee that the influence of the composition and relative size of the mixture components on the position of the second maximum was also noted by Ely⁹ and by Huber and Ely.¹⁰ The simulation gave the correct location of the second maximum, but an approximate method, based on mean density approximation, failed. Second, in 1995, Matteoli and Mansoori¹¹ published an approximate expression for the pair correlation functions in pure liquids and mixtures. This approximate method also failed to show the qualitative behavior of the pair correlation functions reported in this article.¹²

¹ A. Ben-Naim, *Water and Aqueous Solutions* (Plenum, New York, 1979).

² A. Ben-Naim, *Molecular Theory of Solutions* (Oxford University Press,

New York, 2006).

³J. K. Percus and G. J. Yevick, *Phys. Rev.* **110**, 1 (1958).

⁴E. W. Grundke and D. Henderson, *Mol. Phys.* **24**, 269 (1972).

⁵A. A. Broyles, *J. Chem. Phys.* **33**, 456 (1960); **35**, 493 (1961).

⁶G. J. Throop and R. J. Bearman, *J. Chem. Phys.* **42**, 2838 (1965); **44**, 1423 (1966).

⁷G. J. Martyna, D. J. Tobias, and M. L. Klein, *J. Chem. Phys.* **101**, 4177

(1994).

⁸J. K. Johnson, J. A. Zollweg, and K. E. Gubbins, *Mol. Phys.* **78**, 591 (1993).

⁹J. F. Ely, *Int. J. Thermophys.* **7**, 381 (1986).

¹⁰M. L. Huber and J. F. Ely, NIST Technical Note No. 1331, 1989.

¹¹E. Matteoli and G. A. Mansoori, *J. Chem. Phys.* **103**, 4672 (1995).

¹²E. E. Matteoli, personal communication (July 20, 2005).

